Journal of Colloid and Interface Science 448 (2015) 339–346

Contents lists available at ScienceDirect

Journal of Colloid and Interface Science

www.elsevier.com/locate/jcis

Interaction of *Moringa oleifera* seed protein with a mineral surface and the influence of surfactants

Habauka M. Kwaambwa [a,*], Maja S. Hellsing [b], Adrian R. Rennie [b,*], Robert Barker [c]

[a] Polytechnic of Namibia, School of Health and Applied Sciences, Private Bag 13388, 13 Storch Street, Windhoek, Namibia
[b] Materials Physics, Department of Physics and Astronomy, Ångström Laboratory, Uppsala University, Box 516, 751 20, Uppsala, Sweden
[c] Institut Laue Langevin, 71 avenue des Martyrs, CS 20156, 38042 Grenoble Cedex 9, France

GRAPHICAL ABSTRACT

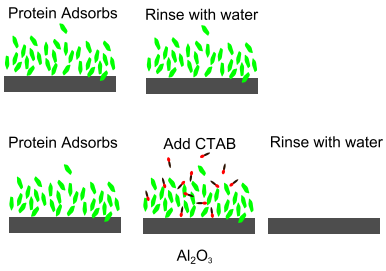

ARTICLE INFO

Article history:
Received 20 December 2014
Accepted 11 February 2015
Available online 23 February 2015

Keywords:
Cetyltrimethylammonium bromide
Moringa oleifera
Neutron reflection
Reflectivity
Sapphire
Seed protein
Sodium dodecylsulfate
Surface excess

ABSTRACT

The paper describes the adsorption of purified protein from seeds of *Moringa oleifera* to a sapphire interface and the effects of addition of the anionic surfactant sodium dodecylsulfate (SDS) and the cationic surfactant hexadecyltrimethylammonium bromide (CTAB). Neutron reflection was used to determine the structure and composition of interfacial layers adsorbed at the solid/solution interface. The maximum surface excess of protein was found to be about 5.3 mg m^{-2}. The protein does not desorb from the solid/liquid interface when rinsed with water. Addition of SDS increases the reflectivity indicating co-adsorption. It was observed that CTAB is able to remove the protein from the interface. The distinct differences to the behavior observed previously for the protein at the silica/water interface are identified. The adsorption of the protein to alumina in addition to other surfaces has shown why it is an effective flocculating agent for the range of impurities found in water supplies. The ability to tailor different surface layers in combination with various surfactants also offers the potential for adsorbed protein to be used in separation technologies.

1. Introduction

Protein adsorption to surfaces is common in many biological and industrial processes. Knowledge of the mechanism of adsorption and the structure of the adsorbed protein layers is important in areas relevant to biology (protein chromatography, cellular adhesion), medicine (biomedical materials), food processing (stabilization of foams and emulsions, fouling of equipment) and biotechnology [1]. Protein adsorption is a common phenomenon; wherever proteins come into contact with a solid interface, they are very likely to adsorb to it. The adsorption phenomena of protein molecules include a number of interactions at solid–liquid interfaces [2,3]. To understand the interaction between protein molecules and solid surfaces it is important to consider many factors,

* Corresponding authors.
E-mail addresses: hkwaambwa@polytechnic.edu.na (H.M. Kwaambwa), Adrian.Rennie@physics.uu.se (A.R. Rennie).

http://dx.doi.org/10.1016/j.jcis.2015.02.033
0021-9797/

such as the physical and chemical properties of solid surfaces for example the roughness and chemical dissociation, properties of the protein molecules like the folding and isoelectric point, and the solution conditions for the protein [4]. Many proteins are amphiphilic because they contain a mixture of amino acids with hydrophobic chains and ionic or polar side chains. They aggregate in solution and may be surface active even at very low concentrations.

This study addresses the adsorption from dilute aqueous solution of protein extracted from *Moringa oleifera* (MO) seeds to aluminum oxide surfaces. There is a large body of literature investigating the MO protein as an effective flocculating agent in water purification [5–9]. Although the details of the mechanism of water purification are not yet well understood, there is evidence that the role of the protein is directly related to adsorption [10,11]. There are general reviews about the chemistry of *Moringa* products that also relate to economic and environmental issues [12,13]. Information on the amount of material that is adsorbed at the surface, the structure of the adsorbed layer and how this relates to concentration in solution is obviously of crucial importance in making efficient use of the protein and providing water with low levels of both impurities and additives. To understand the adsorption mechanism, well-defined interfaces are required to avoid any ambiguity originating from the substrate surface. The binding of a water purification protein to silicon oxide (SiO_2) and its interaction with an anionic surfactant sodium dodecylsulfate (SDS) has been investigated previously using neutron reflection over a range of solution conditions with different concentrations of surfactant using an in-situ solid/liquid adsorption cell [10]. This technique is able to measure not only the adsorbed amounts but also provides information about the surface/interfacial structure of the adsorbed protein at a resolution that cannot be obtained currently using other methods. Interaction of adsorbed proteins with surfactants is of interest as displacement of functional layers may be significant. In the case of water treatment, natural surfactants may occur in the water to be treated. In food applications, stabilization of foams and emulsions may depend on the interaction of proteins, as steric stabilizers, with other surfactants.

The use of the *Moringa* seed protein as a flocculating agent and the unusual dense flocs with a high fractal dimension that are formed has been studied using small-angle and ultra small-angle neutron scattering [14]. Results were discussed primarily in the context of water purification. The present work has been designed to investigate the range of materials that will interact with the protein and thus removed in a purification process. The study with added surfactants suggests how selectivity of adsorption can be achieved and could be exploited in processes such as separation of different types of particles, for example in mineral processing.

Crystals of sapphire (α-Al_2O_3) are convenient substrates for studies of adsorption to alumina because it has an advantageous combination of optical and mechanical properties e.g. [15,16]. The chemical properties of sapphire surfaces are important factors when the surfaces are brought into contact with an aqueous solution [17–20]. For the present study, sapphire was chosen as a good model for a mineral surface that does not have strong negative charge in a solution at neutral pH. The isoelectric point (iep) of alumina, which is the pH at which the surface has a net charge of zero, is reported in literature to be between pH 6–8.5 and depends on the crystal plane [21]. This is close to neutral pH which makes it easy to achieve either a positively or negatively charged surface. Silica, SiO_2, another commonly used substrate for surface adsorption studies has an iep of about 2, making only a neutral or negatively charged surface practically available. The study by Isono et al. [22] has reported the point of zero charge for single-crystal sapphire to be below pH 7. The surface charge arises from deprotonation and protonation of hydroxyl groups on the surface. Measurements of the contact angle of water show that the sapphire surface is macroscopically hydrophilic [21].

This paper reports the results of adsorption of MO protein to sapphire substrates and the effect of added surfactant using neutron reflection. We have recently studied the adsorption of different surfactants to sapphire [17–20]. In the present study, the surfactants were chosen as simple proxies for materials that might occur in real applications and we used sodium dodecylsulfate (SDS) and cetyltrimethylammonium bromide (hexadecyltrimethylammonium bromide or CTAB), which are anionic and cationic, respectively. In a previous study of the adsorption of the MO protein on SiO_2, SDS was found to co-adsorb to the irreversibly bound protein layer [10]. The SDS did not displace the protein even at a concentration above the critical micelle concentration (cmc). The adsorbed layer of protein apparently binds SDS into a denser layer at the surface. Although the protein has a net positive charge and is thus likely to bind to a negatively charged silica surface, SDS does not simply cause desorption by neutralizing the protein.

2. Experimental principles and interpretation of neutron reflection data

Neutron reflectometry is widely used to study adsorption on flat solid substrates and at air–liquid interfaces [23,24]. The measured signal depends on the variation of the refractive index, n, in the direction perpendicular to the surface. The experiment involves determination of the reflectivity of an interface as a function of the wavelength or angle. The data allows quantitative, structural, and compositional information about the adsorbed material to be obtained at molecular length scales. In specular neutron reflection, the ratio of the intensity of the reflected beam to that of the incident beam is measured as a function of the momentum transfer, Q normal to the reflecting surface. The specular condition occurs when the angle of the incident beam is equal to the angle of the reflected beam and Q is given by

$$Q = (4\pi/\lambda)\sin\theta \tag{1}$$

where λ is the incident neutron wavelength and θ is the angle of incidence. Measurements can be made using combinations of different wavelengths and incident angles. The scattering is a nuclear interaction, and information is derived via the scattering length density of the materials, given by

$$\rho = \sum N_i b_i \tag{2}$$

where N_i is the number density of the element or isotope i, and b_i is the coherent neutron scattering length of the species. The scattering length density, ρ, determines the refractive index, n, for the neutrons, which is given by:

$$n = 1 - (\lambda^2/2\pi)\rho \tag{3}$$

A particular advantage of neutron reflection is that b can vary between isotopes of an element and there is a large difference for normal hydrogen (^{1}H) and deuterium (^{2}H or D). Table 1 shows the scattering length densities of materials used in the present study. By matching ρ for the solvent with that of the substrate, one can obtain a reflection signal that depends only on the interfacial layer. Making additional measurements with different hydrogen and deuterium composition in the solvent allows one to verify the composition of surface layers as ρ is related to the volume fraction of each component in the layer by

$$\rho = \phi_p\rho_p + \phi_w\rho_w \tag{4}$$

and the constraint $\phi_p + \phi_w = 1$ is used. ρ_p and ρ_w are the scattering length densities of protein and water, respectively, and ϕ_p and ϕ_w are their respective volume fractions. If a protein molecule has a

Table 1
Properties of materials used.

Material	Chemical formula	Density ($g\ cm^{-3}$)	Scattering length density (10^{-6} Å^{-2})
Water	H_2O	0.997	−0.56
Heavy water	D_2O	1.105	6.35
Alumina	Al_2O_3	3.98	5.71
Moringa protein (in H_2O)		1.35	1.46
Moringa protein (in D_2O)		1.36	2.60
Sodium dodecylsulfate (SDS)	$NaC_{12}H_{25}SO_4$	1.01	0.34
Deuterated sodium dodecylsulfate (d-SDS)	$NaC_{12}D_{25}SO_4$	1.10	5.83
Hexadecyltrimethylammonium bromide (CTAB)	$C_{16}H_{33}N(CH_3)_3Br$	1.14	−0.35

total scattering length b_p (from the sum of b_i for all component atoms), the area per molecule, A, and the interfacial layer of thickness, t_L, are related by

$$A = b_p/(t_L\phi_p\rho_p) \quad (5)$$

These equations can be extended readily to layers that consist of mixtures of different components, such as surfactants with protein or to multiple layers with gradual changes of composition [17]. If an adsorbed surfactant is modeled as a single layer and the molecule has a total scattering length b_s (from the sum of b_i for all component atoms), the area per molecule, A, in an interfacial layer of thickness, t_L, can be can calculated using Eq. (5) above.

The surface excess, Γ, in mass per unit area can be obtained from

$$\Gamma = M_W/AN_A \quad (6)$$

where M_W is the molecular mass of the adsorbate and N_A is Avogadro's constant.

The reflectivity for an interface can be calculated using conventional methods of optics with a recursive matrix algorithm that divides the structure into layers of defined refractive index and thickness, t. It is also straightforward to include a small amount of roughness or mixing of components between adjacent layers using an approximation for a Gaussian height profile at the surface [23].

The experimental advantages of neutron reflection include the ability to measure buried interfaces such as those between a crystal and a liquid. Neutron beams are attenuated little on passing through single crystals and the transmission of 50 mm of sapphire is about 60% for the wavelengths used in the present study. In these experiments, the beam passes through a crystal, entering at almost normal incidence on a flat face, and then reflecting at a glancing angle from an internal surface. The reflecting face of the crystal is clamped against a PTFE seal that retains the solution of interest so as to provide information about the adsorbed layers at the solid/liquid interface. Details of geometry and cell design have been provided in previous papers [25,26].

As neutron reflection measures directly macroscopic interfaces, it can be applied to investigate adsorption for systems that are not stable colloids. It can therefore be used to provide quantitative information about the structure of interfacial layers over a wide range of external conditions. Measurements with different contrasts of solvent or by labeling parts of surfactant molecules allows the relative amounts of different components in layers near a surface to be determined.

3. Materials

SDS 'Sigma Ultra grade' (cmc in H_2O at 25 °C = 8.2 mM) and CTAB (cmc in H_2O at 25 °C = 0.92 mM) were purchased from Sigma–Aldrich and Fluka, respectively, and were both used without further purification. For the neutron experiments, water was obtained from a Millipore system and heavy water, D_2O, was supplied by EURISO-TOP, CEA, Saclay. The MO seeds were obtained from suppliers in Botswana and Zambia and were stored at room temperature prior to extraction of the protein as described in previous papers [27–30]. Protein solutions were prepared by tumbling overnight. The pH (pD) of 0.2 wt% solutions were found to be in the range 6–6.8.

4. Experimental methods

4.1. Measurement procedures and characterization of the substrate

Measurements were made on the surface of a single crystal of sapphire, Al_2O_3. Prior to use, the sapphire substrate was cleaned with dilute 'Piranha' solution (aqueous mixture using volume fractions 0.1 of H_2O_2 (30 wt% in water), 0.4 H_2SO_4 (conc. 96.0%) and 0.5 H_2O at a temperature of between 70 and 80 °C for 15 min. *Note that although this reagent is less aggressive than the usual 'Piranha solution', protective equipment and clothing are essential.* The mixture removes organic impurities from the substrate surface. The surface was then rinsed extensively with 'Millipore' pure water. The cleaning procedure is important as it may affect the substrate surface chemistry. The substrates used for the data reported here were all cleaned in the same way and characterized by neutrons prior to adsorption. The other parts of the cell and connecting tubing were cleaned with Decon 90™, followed by extensive rinsing with pure water.

The neutron reflectivity experiments were performed on the reflectometer D17 at the Institut Laue Langevin, Grenoble (France) [31,32]. The time-of-flight (TOF) mode used neutron wavelengths between 2 and 24 Å to provide reflectivity data over a wide range of Q simultaneously. The average Q resolution was approximately 5% in the current measurements. Data were recorded at two incident angles of 0.8° and 3.2°, with collimating slits varied accordingly to ensure a constant footprint on the sample. Depending on the intensity of reflectivity measured, this permitted collection of reflectivity in the range of Q from about 0.0075 to 0.25 Å^{-1}, although few samples showed significant measurable signal beyond 0.2 Å^{-1}.

The PTFE gasket between the crystals was machined so that connectors for tubing from a Knauer Smartline 1000 HPLC pump with Smartline Manager 5000 degasser unit could be attached to fill and flush the sample cell automatically. The pump was programmed to inject specific mixtures from appropriate stock solutions. The volume of the cell is about 3 mL, and in these experiments, 10 mL of each solution was flushed through the cell with a flow-rate of 2 mL min^{-1} to ensure complete exchange of the sample.

4.2. Model fitting

Neutron reflectivity, in common with other scattering techniques such as small-angle scattering, cannot always yield a unique structure from direct inversion of the data. The reflectivity curve is instead fitted with a model scattering length density profile consisting of the layer compositions and thicknesses, along with the shape of the interfacial mixing profiles between layers in the film. In practice, one must utilize as much ancillary information as possible to constrain the model used to fit the neutron reflectivity curve, as it is possible to fit a data set simply by adding more model parameters. The key to robust structural characterization is to construct scattering length density profiles consistent with multiple measurements of the same sample with the minimum number of adjustable parameters needed for a good fit. All

fits shown in this manuscript were made using the program cprof [33].

5. Results and discussion

5.1. Characterization of the substrate

Experiments were carried out to check the substrate cleanliness and to characterize the interface before further studies of adsorption were made of the protein and protein-surfactant mixtures. To characterize the sapphire surface, reflectivity profiles were first measured in pure water with different isotopic contrasts 50% D_2O, H_2O and D_2O in this order, a typical data set is shown in Fig. 1. A model was found in a combined fit of the three contrasts for reflection data in the range of Q from 0.008 to 0.15 $Å^{-1}$ for 50% D_2O and H_2O contrasts and only up to Q equal to 0.032 $Å^{-1}$ for D_2O due to the low signal seen at larger Q. A summary of the densities and scattering lengths of the materials is provided in Table 1. The sapphire substrate was found to have a surface layer with about 15% reduced density over a thickness 15 ± 2 Å with a solvent fraction of about 20% in the outer 5 Å of this layer. A roughness of 4 Å at the sapphire surface was included in the fit of the clean substrate. These parameters were used for the substrate in the models of the adsorbed protein.

5.2. Adsorption of protein on sapphire

Neutron reflection experiments were used to measure the adsorption of the MO seed protein to sapphire both in the absence of surfactant as well as with added SDS and CTAB. The MO protein is clearly seen to adsorb to sapphire as the measurements showed changes of reflectivity and a pronounced fringe appears as the concentration of protein increased as shown in Fig. 2. This adsorption reaches a plateau for concentrations between 0.05 and 0.2 wt%. It was possible to rinse the surface of adsorbed protein with pure D_2O without significantly changing the reflectivity, see below. This allowed measurements with other contrasts of water (H_2O) for the concentration of 0.2 wt% and thus a structural model for the layer could be established. The fit shown in Fig. 2 corresponds to the structure of the sapphire interface described previously with two additional layers of hydrated protein and then a continuous exponential decay of protein density toward the bulk solution. In this analysis, the scattering length density of the layers that represent hydrated protein are allowed to vary between that for the protein in the appropriate solvent allowing for proton exchange and

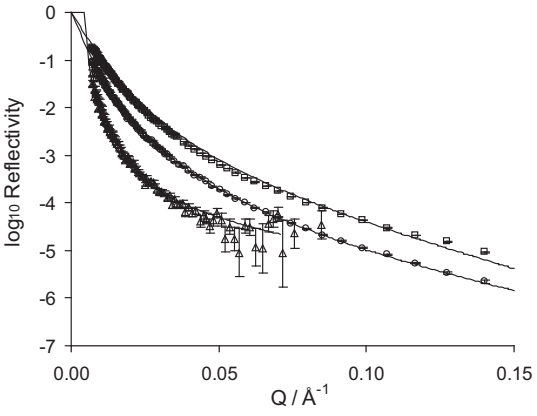

Fig. 1. Reflectivity data for the clean sapphire substrate in different contrasts of water: □ H_2O, ○ 50% D_2O and Δ D_2O. The solid lines are calculated using a layer thickness of 15 Å.

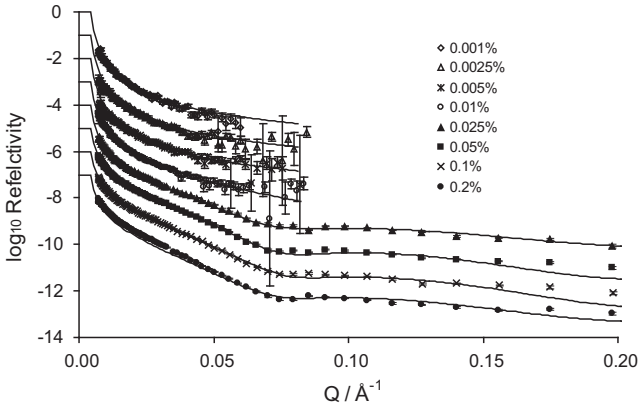

Fig. 2. Neutron reflectivity data for the MO protein at concentrations from 0.001 to 0.2 wt% on a sapphire surface in D_2O. The solid lines are the typical fits of the reflectivity data (the error bars are sometimes smaller than the data point symbols). Each data set is offset on increasing concentration by 10^{-1} for clarity.

that of the pure solvent. The volume fraction is calculated from the known material properties listed in Table 1. The parameters for the combined fit are shown in Table 2. The diffuse structure at the solution interface is represented by an exponential decay of protein density away from the surface as such large inhomogeneous regions are not well represented by a small roughness. A roughness of 5 Å was included between the protein layers 1 and 2 in all the model curves.

The model corresponds to an adsorbed amount of 5.3 ± 0.5 mg m^{-2} with a volume fraction of protein of 0.52 near the surface, 0.38 further out in a second layer, which then decays exponentially to zero. The uncertainty has been estimated as a combination of the statistics of counting giving rise to deviations in the fitted functions and systematic errors. These estimates are shown in the tables of fit parameters. Other functions for the protein density with broadly similar shape could also fit the data but neither the amount at the surface nor the overall length scales are changed significantly in these models.

The density profile of the protein calculated from the fit is shown in Fig. 3 and the adsorption isotherm is similar to that seen at SiO_2 surface previously [10,11] in that the structure of the layer in equilibrium with protein solution is similar. However, the adsorbed amount is considerably higher at the SiO_2 surface for the same protein concentration. For comparison, the adsorption data from the previous studies on silica and on polystyrene latex particles are also shown in Fig. 3.

Although the availability of neutron beam time precluded the measurements of multiple contrasts for all concentrations of protein, the adsorption isotherm for the protein in pure water (D_2O) was determined (see Fig. 3). In this contrast, the reflected signal is dominated by the amount of adsorbed interfacial material, which allows surface excess to be determined readily. The data shows that there is a plateau in the surface excess at about 5.5 mg m^{-2}. The adsorption of the protein on silica may be ascribed to electrostatic interaction between the positively charged protein and the negatively charged surface. As the sapphire, in contrast to silica, will be close to the iep at pH 7 the driving force for adsorption is likely to be different.

5.3. Effect of rinsing with water

Measurements were made to investigate whether the protein could be displaced with either water or surfactants. As the difference of scattering length density between D_2O and sapphire is small, although not perfectly matched, the overall level of

Table 2
Fit parameters for the protein layer in water with concentration 0.2 wt%.

Layers contrast	Protein layer 1 thickness (±2 Å) Å	ρ for layer 1 (±0.2 10^{-6} Å^{-2}) 10^{-6} Å^{-2}	Protein layer 2 thickness (±2 Å) Å	ρ for layer 2 (±0.2 10^{-6} Å^{-2}) 10^{-6} Å^{-2}	Exponential decay length (±2 Å) Å
D_2O	35	4.6	33	5.1	22
H_2O	35	0.8	33	0.4	22

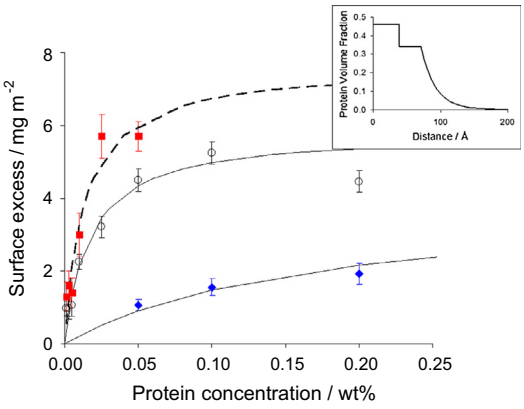

Fig. 3. Adsorption isotherm of MO seeds protein in pure D_2O to sapphire (○) deduced from the neutron reflectivity data and fits (parameters shown in Table 3). For comparison the adsorption measured in previous studies to silica [10] (■) and to polystyrene latex [14] (♦) are also shown. The inset shows the protein volume fraction profile for the highest concentration of protein on sapphire.

reflectivity for measurements of solutions in D_2O provides a simple indication of the amount of hydrogenous material at the interface.

Fig. 4 shows the effect of rinsing pre-adsorbed protein on sapphire with 20 mL of D_2O. Since the curves before and after rinsing overlap, it is clear that the protein is not removed by flushing the cell with D_2O. A similar irreversible adsorption behavior was observed in the experiments carried out previously by Kwaambwa et al. [10] for an adsorbed layer of *M. oleifera* protein on a silica substrate after rinsing with water.

5.4. Effect of adding SDS at different concentrations

Fig. 5 shows the effect of exposing the pre-adsorbed protein layer to successively higher concentrations of SDS in D_2O. At lower SDS concentrations (i.e. 0.12, 0.24 and 0.48 mM), the curves overlap. In comparison, when adding SDS to a protein layer adsorbed on silica surface, co-adsorption was apparent at lower concentrations (certainly by 0.24 mM) [10]. However, the data indicate that there are significant changes in the adsorbed layer for surfactant solution concentrations of 0.96 mM and above. Significant effects are visible even well below the critical micelle concentration (CMC), 8.8 mM, of the surfactant. This effect is clear from the data where the reflectivity is increased and the fringe in the reflectivity is less pronounced. The observed effect of SDS is in agreement with previous physical measurements by Maikokera and Kwaambwa of surface tension [27,28], fluorescence [29], circular dichroism [30] and viscosity [34] when studied as function of SDS surfactant concentration for 0.05 wt% protein solution. All measurements exhibited either maximum or minimum at a critical SDS concentration of about 1 mM.

Rinsing the sample with water after exposure to SDS reduces the change seen when SDS was added. This suggests that some material is removed upon rinsing. Neutron reflection measurements with only one solvent contrast in D_2O do not allow unambiguous distinction as to whether it is the protein or surfactant that is removed, or some of both.

Approximate fits to the data for 0.96 and 2 mM SDS can be made with layers that have the same thickness as in the sample with no SDS. The scattering length density is lower than that of the layers of protein. If one assumes that the protein remains with an unchanged distribution, then it is easy to estimate the amount of SDS in the layers. The results for fits to the data are shown in Table 4. Using the same model, when constrained in the same way to the 12 mM SDS data, the fit is poor and not physically meaningful. For the 12 mM SDS data a better model to fit data is obtained with a thinner, denser layer, near the sapphire surface. When the 12 mM SDS sample was rinsed with D_2O, the reflectivity curve does not resemble either the data from protein with SDS measured before rinsing or the original adsorbed protein layer. The reflectivity after final rinsing with D_2O is very low which suggest that some material is removed that could be either protein or SDS.

The changes in the adsorbed protein layer with SDS at the higher concentrations are shown in more detail in Fig. 6. The experimental protocol involved rinsing the protein adsorbed on

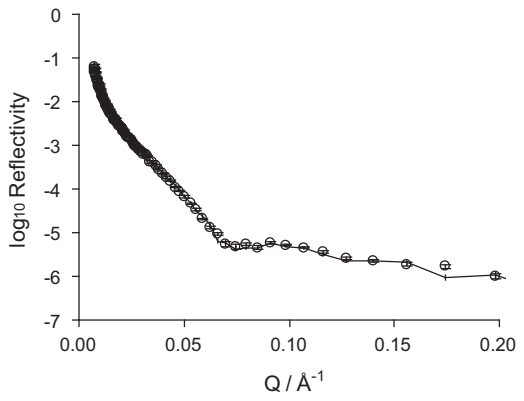

Fig. 4. Effect of rinsing adsorbed protein on sapphire, after exposure to a solution of 0.05 wt% protein (○), with pure water, D_2O (continuous line).

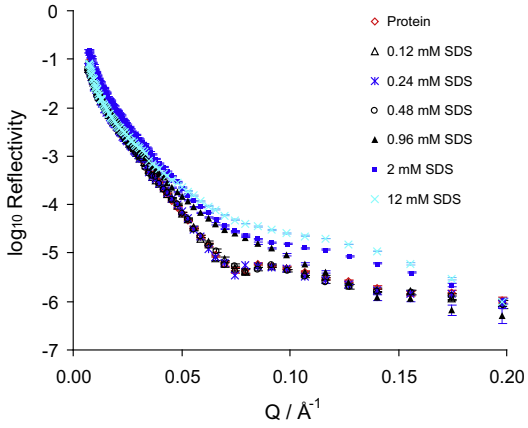

Fig. 5. Effect of addition of SDS at different concentrations to a pre-adsorbed layer of MO protein (solutions in D_2O).

Table 3
Fit parameters for the protein in D_2O at various concentrations.

Protein concentration wt%	Protein layer 1 thickness (±2 Å) Å	ρ for layer 1 (±5%) 10^{-6} Å^{-2}	Protein layer 2 thickness (±2 Å) Å	ρ for layer 2 (±5%) 10^{-6} Å^{-2}	Exponential decay length (±2 Å) Å	Γ (±10%) mg m^{-2}	Volume fraction – near surface ± 0.05
0.001	14	4.4	42	6.0	12	1.7	0.52
0.025	24	4.6	40	5.6	13	3.1	0.46
0.01	14	4.0	44	5.9	11	2.2	0.62
0.05	22	4.4	39	5.2	22	4.5	0.52
0.1	37	4.6	30	5.1	23	5.2	0.46
0.2	39	4.6	32	5.1	21	5.3	0.46

Table 4
Fit parameters for the protein/SDS in D_2O-based on joint fit to all contrasts.

SDS concentration mM	Thickness adsorbed layer 1 (±2 Å) Å	ρ layer 1 (±0.2 10^{-6} Å^{-2}) 10^{-6} Å^{-2}	Thickness adsorbed layer 2 (±2 Å) Å	ρ layer 2 (±0.2 10^{-6} Å^{-2}) 10^{-6} Å^{-2}	Length (±2 Å) Å	ϕ_1 SDS (±0.02)	ϕ_2 SDS (±0.01)
0.96	36	3.96	32	5.03	24	0.11	0.01
2	36	3.38	32	4.44	24	0.21	0.10

sapphire first with a solution of SDS in D_2O, followed by pure D_2O (Fig. 6) and pure H_2O (supporting information Fig. S1). The addition of 12 mM SDS increases the reflectivity and the sharp fringe diminishes which is indicative of the disappearance of a thick, well-defined layer. Rinsing with D_2O causes the curve to move toward that observed for the clean sapphire/D_2O interface but it does not overlap with the data for a clean interface.

Additional measurements with SDS prepared with the alkyl chains substituted fully with deuterium in place of normal hydrogen, provided by the Oxford deuteration laboratory allow us to confirm that there is some adsorption or binding of SDS to the protein layer. The data are shown in the supporting information (Fig. S2). Consistent fits to all the contrasts could be made under the assumption that the amount of adsorbed protein is unchanged when the surfactant solution is present, models with profiles similar to those described above with some SDS.

5.5. Effect of adding CTAB at different concentrations

A similar series of measurements were made to study the interaction of the cationic surfactant CTAB with a layer of pre-adsorbed protein. The data for measurements of solutions in D_2O are shown in Fig. 7.

When a solution of 9.0 mM CTAB dissolved in D_2O is added, higher reflectivity is observed and the fringe disappears similar to that observed for protein with a SDS solution, suggesting that a dense, thinner layer is formed. The CMC of CTAB in pure water is 0.9 mM and so this concentration corresponds to 10 × CMC. Unfortunately with the data available for just one contrast, it is not possible to identify whether the surfactant has displaced entirely the protein from the interface and formed its own adsorbed interfacial layer or whether there is some protein remaining. Further rinsing of the substrate with D_2O causes the reflectivity to drop and the data overlaps with that observed for the clean sapphire/D_2O interface, shown in Fig. 8 (supporting information Fig. S3 shows data for a further rinse with H_2O). This indicates that the adsorbed protein may have been removed by the process of rinsing first with CTAB and then with D_2O. The behavior of protein being displaced completely after rinsing with CTAB and then with water is in contrast to the behavior with SDS.

5.6. Comparison with different adsorption substrates

It is interesting to compare the observations reported here with the recent study of adsorption of MO protein at the silica-solution interface (see Fig. 3) as well as considering the behavior of the pure surfactants at the sapphire solution interface [10]. At the silica

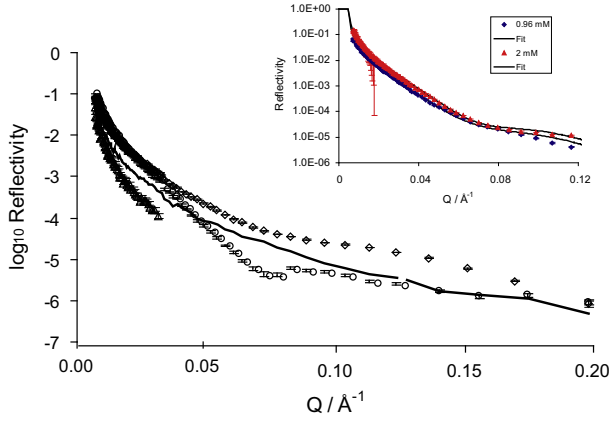

Fig. 6. Reflectivity of pure D_2O (Δ), 0.2 wt% solution of MO protein in D_2O (○) and with 12 mM SDS/D_2O (◇), and after rinsing with 20 mL of D_2O (solid line). The parameters and the derived amount of SDS are shown in Table 4, the inset shows the fits to the 0.96 and 2 mM SDS data.

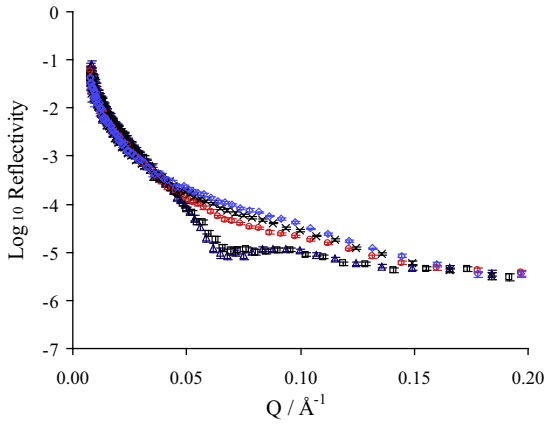

Fig. 7. Effect of added CTAB at different concentrations to a pre-adsorbed layer of MO protein (solutions in D_2O); Δ 0.2% protein, □ 0.3 mM CTAB, ○ 0.9 mM CTAB, × 2.7 mM CTAB, ◊ 9.0 mM CTAB.

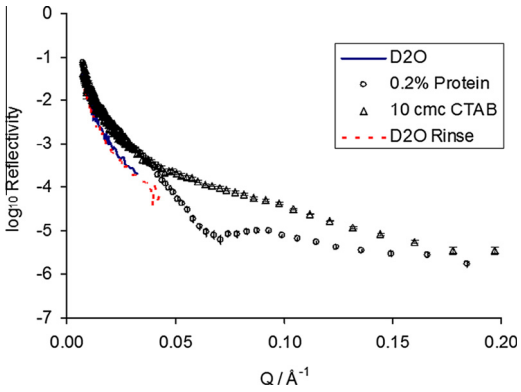

Fig. 8. Reflectivity of pure D_2O (solid line), 0.2 wt% solution of MO protein in D_2O (○) and in 10 mM CTAB/D_2O (Δ) and after rinsing with 20 mL of D_2O (dashed line).

interface, SDS was seen to penetrate into the protein layer and co-adsorb. The protein was not displaced by rinsing with water and was seen to extend through a thick region that corresponded approximately to the thickness of the protein layer. At neutral pH, SDS does not adsorb to silica but does adsorb to the sapphire surface as a thin, dense layer [20].

At the sapphire surface, the *Moringa* protein can be removed by rinsing with either SDS or CTAB and then with water. The CTAB is seen to cause desorption of all the protein leaving a bare clean surface after rinsing. However, in the case of SDS, flushing with a small amount of water does not remove all of the adsorbed material. It is however known that SDS does bind to sapphire and it is not displaced by water and so it is likely that it is co-adsorbed more strongly.

5.7. Comparison of interaction with different surfactants – relation to applications

The *Moringa* seed protein on its own binds to a broad range of different materials – these can have very different polarity and isoelectric points. Although at neutral pH the protein is cationic, the range of pK_a for the different amino acids can give rise to various ionic association as well as hydrophobic interactions. Interaction with surfactants is interesting in relation to various current and potential applications. In water purification there can be a range of contaminants in the supply and it is important that natural surfactants would not alter significantly the tendency to act as a flocculating agent. The experiments with SDS suggest that anionic surfactants that are widespread would leave some material adsorbed to alumina as found previously with silica [10].

Cationic surfactants have a range of specific applications such as in mineral processing. It is apparent that the interaction of CTAB with alumina is sufficient to displace the protein. The surfactant can then be removed by rinsing with pure water. The possibility to tailor a combination of protein and appropriate surfactants to modify the surface of specific oxides so as to have different interactions suggests a means to develop separation methods for different minerals. This should be the subject of further studies.

6. Conclusions

The adsorption of MO seed protein to alumina has been studied using neutron reflection. A diffuse layer of protein that extends from a denser but hydrated layer near the surface is observed. A plateau in the adsorbed amount is reached for concentrations above 0.1 wt%. This structure is similar to that reported for the adsorption on silica [10]. There is however an important distinction between the two interfaces: on alumina the protein is not bound strongly to the interface and could be readily displaced whereas for the silica surface, the protein was seen to be irreversibly bound. For example, rinsing with solutions of the anionic surfactant SDS and water could remove most of the adsorbed protein. Exposure to the cationic surfactant CTAB provided essentially a clean substrate.

Norde and Lyklema [35] have provided a review of the binding of globular proteins to interfaces and comment that adsorption is often irreversible and that a plateau is usually reached when molecules are close-packed at the interface. The present work provides interesting and contrasting results: the neutron reflection results indicate clearly that the thickness and the amount of material corresponds to several adsorbed molecules with a total thickness larger than a single molecule. An important distinction between *M. oleifera* seed protein and the immunoglobulins is that MO has a marked tendency to associate in solution although at low concentrations, up to 0.2 wt%, light scattering [36] did not indicate very large aggregates. The results suggest that further comparison of the association in solution and the structure of adsorbed layers will be valuable for proteins under a range of physicochemical conditions.

In applications such as use of *Moringa* seed protein as a flocculating agent for water purification [5], it is important to understand how much material is required for different levels of contamination and different types of impurities. Adding excess that would remain in the water causes not only expense and waste but could cause increased oxygen demand in treated water. The new results will help to guide optimized use in practical applications [12].

The present results demonstrate that the binding of the protein to an interface does depend on the chemical nature of the substrate and is not simply a consequence of the hydrophobic nature of the protein and can depend on favorable interactions with the substrate. The ability of the protein to bind to different oxide surfaces as well as other materials is clearly important in its uses as a flocculating agent that can be used in water treatment. The consequences of displacement of the protein with surfactant from specific particles are interesting for application purposes as this implies that the protein could be used to provide specific and reversible interactions with different particles, for example as an aid in mineral flotation.

Acknowledgments

We acknowledge funding from the University of Botswana, Polytechnic of Namibia and VR/SIDA (research contract No. 348-2011-7241). We are grateful to the ILL for provision of neutron facilities.

Appendix A. Supplementary material

Supplementary data associated with this article can be found, in the online version, at http://dx.doi.org/10.1016/j.jcis.2015.02.033.

References

[1] S. Seeger, M. Rabe, D. Verdes, Adv. Colloid Interface Sci. 162 (2011) 87–106.
[2] W. Norde, T.A. Horbett, J.L. Brash, 'Proteins at interfaces III: introductory overview' in proteins at interfaces III State of the Art, in: T. Horbett, et al. (Ed.), ACS Symposium Series 2012, American Chemical Society, Washington, DC.
[3] A.G. Richter, I. Kuzmenko, Langmuir 29 (2013) 5167–5180.
[4] T. Ogino, K. Yamazali, T. Ikeda, T. Isono, J. Colloid Interface Sci. 361 (2011) 64–70.
[5] A. Ndabigengesere, K.S. Narasiah, G.B. Talbot, Water Res. 29 (1995) 703–710.
[6] T. Okuda, A.U. Baes, W. Nishijima, M. Okada, Water Res. 35 (2001) 830–834.
[7] S.M.I. Sajidu, E.M.T. Henry, I. Persson, W.R.L. Masamba, D. Kayambazinthu, J. Biotechnol. 5 (2006) 2397–2401.
[8] G. Sarpong, C.P. Richardson, African J. Agric. Res. 5 (2010) 2939–2944.

[9] G.S. Madrona, G.B. Serpelloni, A.M.S. Vieira, L. Nishi, K.C. Cardoso, R. Bergamasco, Water Air Soil Pollut. 211 (2010) 409–415.
[10] H.M. Kwaambwa, M. Hellsing, A.R. Rennie, Langmuir 26 (2010) 3902–3910.
[11] S.B. Velegol, H.A. Jerri, K.J. Adolfsen, L.R. McCullough, D. Velegol, Langmuir 28 (2012) 2262–2268.
[12] J. Shindano, C. Kasase, Moringa (*Moringa oleifera*): a source of food and nutrition, medicine and industrial products. ACS Symposium Series [0097-6156], vol. 1021, 2009, pp. 421–467.
[13] S.K. Kansal, A. Kumari, Chem. Rev. 114 (2014) 4993–5010.
[14] M.S. Hellsing, H.M. Kwaambwa, F.M. Nermark, B.B.M. Nkoane, A.J. Jackson, M.J. Wasbrough, I. Berts, L. Porcar, A.R. Rennie, Colloids Surf. A: Physicochem. Eng. Aspects 460 (2014) 460–467.
[15] T. Ogi, L.B. Modesto-Lopez, F. Iskander, K. Okuyama, Coll. Surf. A: Physicochem. Eng. Aspects 297 (2007) 71–78.
[16] T.A Oleson, N. Sahai, D.J. Wesolowski, J.A. Dura, C.F. Majkrzak, A.J. Giuffre, J. Colloid Interface Sci. 370 (2012) 192–200.
[17] M.S. Hellsing, A.R. Rennie, Langmuir 26 (2010) 14567–14573.
[18] M.S. Hellsing, A.R. Rennie, Langmuir 27 (2011) 4669–4678.
[19] N. Li, R.K. Thomas, A.R. Rennie, J. Colloid Interface Sci. 369 (2012) 287–293.
[20] N. Li, R.K. Thomas, A.R. Rennie, J. Colloid Interface Sci. 378 (2012) 152–158.
[21] G.V. Franks, Y. Gan, J. Am. Ceram. Soc. 90 (11) (2007) 3373–3388.
[22] T. Isono, T. Ikeda, R. Aoki, K. Yamazaki, T. Ogino, Surf. Sci. 604 (2010) 2055–2063.
[23] J. Penfold, R.K. Thomas, J. Phys. Condens. Matter 2 (1990) 1369–1412.
[24] J.R. Lu, R.K. Thomas, J. Penfold, Adv. Colloid Interface Sci. 84 (2000) 143–304.
[25] G. Fragneto, Z.X. Li, R.K. Thomas, A.R. Rennie, J. Penfold, J. Colloid Interface Sci. 178 (1996) 531–537.
[26] G. Fragneto, J.R. Lu, D.C. McDermott, R.K. Thomas, A.R. Rennie, P.D. Gallagher, S.K. Satija, Langmuir 12 (1996) 477–486.
[27] R. Maikokera, H.M. Kwaambwa, Coll. Surf. B 55 (2007) 173–178.
[28] H.M. Kwaambwa, R. Maikokera, Water SA 33 (2007) 583–588.
[29] H.M. Kwaambwa, R. Maikokera, Coll. Surf. B 60 (2007) 213–220.
[30] H.M. Kwaambwa, R. Maikokera, Coll. Surf. B 64 (2008) 118–125.
[31] http://www.ill.fr/YellowBook/D17/.
[32] R. Cubitt, G. Fragneto, Appl. Phys. A 74 (2002) 329–331.
[33] http://material.fysik.uu.se/Group_members/adrian/cprof.htm.
[34] R. Maikokera, H.M. Kwaambwa, Res. Lett. Phys. Chem. 2009 (2009) 1–9, http://dx.doi.org/10.1155/2009/927329. 5 pages, Article ID 927329.
[35] W. Norde, J. Lyklema, Adv. Colloid Interface Sci. 179–182 (2012) 5–13.
[36] H.M. Kwaambwa, A.R. Rennie, Biopolymers 97 (2012) 209–218.